POLITECNICO DI TORINO
Repository ISTITUZIONALE

Assessment of Quadrotor Near-Wall behaviour using six-Degrees of Freedom CFD simulations

(Article begins on next page)

27 April 2024

Assessment of Quadrotor Near-Wall behaviour using six-Degrees of Freedom CFD simulations

5 authors, including:

Manuel Carreño Ruiz
Politecnico di Torino
13 PUBLICATIONS   **39** CITATIONS

SEE PROFILE

Nicoletta Bloise
Politecnico di Torino
19 PUBLICATIONS   **130** CITATIONS

SEE PROFILE

Elisa Capello
Politecnico di Torino
80 PUBLICATIONS   **641** CITATIONS

SEE PROFILE

Domenic D'Ambrosio
Politecnico di Torino
57 PUBLICATIONS   **557** CITATIONS

SEE PROFILE

Some of the authors of this publication are also working on these related projects:

Flying radar View project

Prediction and Simulator Verification of Roll/Lateral Adverse Aeroservoelastic Rotorcraft–Pilot Couplings View project

Assessment of Quadrotor Near-Wall behaviour using six-Degrees of Freedom CFD simulations

M. Carreño Ruiz *, N.Bloise[†], E.Capello[‡], D. D'Ambrosio [§] and G.Guglieri[¶]
Department of Mechanical and Aerospace Engineering, Politecnico di Torino, Torino, 10124, Italy

The growth of Unmanned Aerial Systems (UASs) in various applications requires more autonomous and safe missions. The paper introduces an innovative approach that combines the Computational Fluid Dynamics (CFD) model and closed-loop control algorithm to simulate UAS maneuvers precisely. This study proposes a Proportional-Integrative-Derivative (PID) controller for both position and attitude dynamics due to its simple implementation and employment in a commercial autopilot system. Thanks to the numerical simulation of the UAS aerodynamics, it was possible to perform an accurate analysis, especially for critical conditions, such as wall effect or rapid wind gusts. In these particular situations, it is essential to exploit an advanced propulsive model to capture the interaction between vehicle dynamics, aerodynamics, and environmental conditions. The complete CFD/PID framework enables a virtual testing environment for UAS platforms. The paper compares an innovative in-the-loop CFD approach and a classical simplified propulsive model that adopts constant thrust and torque coefficients to verify the numerical model. Furthermore, we present numerical simulations of a quadcopter in the neighborhood of a wall studying the ability of the discussed control algorithm to maintain a hovering position at different distances from the wall.

I. Introduction

$\mathbf{I}$N recent years, Unmanned Aerial Systems (UASs) have had significant growth in many sectors, as presented in detail in [1], such as in urban air mobility (for example, in smart-cities [2]), as well as in agriculture (for example, in precision operations [3]). Thanks to the progress in robotics, communication, and Big Data, all these UAS missions can guarantee the highest level of automation and safety, as discussed in [4].

Therefore, interdisciplinary researchers are required to respond to all opportunities and challenges. In particular,

---

*PhD Candidate, Department of Mechanical and Aerospace Engineering, Politecnico di Torino, C.so Duca degli Abruzzi, 24, 10124 Torino, Italy, manuel.carreno@polito.it

[†]PhD Candidate, Department of Mechanical and Aerospace Engineering, Politecnico di Torino, C.so Duca degli Abruzzi, 24, 10124 Torino, Italy, nicoletta.bloise@polito.it

[‡]Associate Professor, Department of Mechanical and Aerospace Engineering, Politecnico di Torino, C.so Duca degli Abruzzi, 24, 10124 Torino, Italy, and CNR-IEIIT, Corso Duca degli Abruzzi, 24, 10129 Torino, Italy elisa.capello@polito.it

[§]Adjunct Professor, Department of Mechanical and Aerospace Engineering, Politecnico di Torino, C.so Duca degli Abruzzi, 24, 10124 Torino, Italy, domenic.dambrosio@polito.it

[¶]Full Professor, Department of Mechanical and Aerospace Engineering, Politecnico di Torino, C.so Duca degli Abruzzi, 24, 10124 Torino, Italy and CNR-IEIIT, Corso Duca degli Abruzzi, 24, 10129 Torino, Italy, giorgio.guglieri@polito.it

the performances of multicopters with small inertia are significantly affected by disturbances that could jeopardize the entire mission. The previous studies focused on analyzing disturbances induced by aerodynamic effect, using an Active Disturbance Rejection Control (ADRC) to maintain stability even in the presence of external disturbances, as in [5]. In [6, 7], authors present a disturbance rejection mechanism for Micro Air Vehicles (MAV) based on two control algorithms that switch on according to the process. Likewise, other authors [8] investigate the position and attitude control in environments with extreme external disturbances, such as wind gusts. They present a robust adaptive controller with an aerodynamics, wind gust, and control model integrated into a six-degree-of-freedom UAS dynamics solver. In both the previous works, a Proportional–Integral–Derivative (PID) controller is tuned by adding another adaptive control term, and in[9], an optimized PID is combined to improve disturbance rejection.

Nowadays, the interest in evaluating the flight in the proximity of the ground or walls is significant for several applications in buildings or obstacle areas, such as inspection, delivery, and spraying operations. Also, in these cases, the vehicle is suffered from external forces and torques due to aerodynamic effects, which may cause serious accidents. Therefore, for autonomous navigation in near-surface conditions, the system requests excellent sensing and control algorithm. Meanwhile, introducing aerodynamic proximity effects to tune the control law is an exceptional advantage in avoiding accidents and for general safety. A review of the ground effect on multirotor is presented in[7], and an obstacles effect of crops in a greenhouse is analyzed in [10]. In[11], authors assess the effect of the ground proximity on the drone performance at different flight velocities. The wall effect is also the focus of the research activities presented by [12, 13]. These studies experimentally show the forces and moments sustained by the UAS at several wall distances. These results could become essential data to develop a model that includes this effect. Also, a numerical investigation is presented in [14], focusing on the disturbance phenomena due to aerodynamic interactions between rotors and nearby walls.

Our research introduces a noticeable novelty in this overview, which is the combination of a Computational Fluid Dynamics (CFD) solver to evaluate the state of the UAS using a closed-loop feedback control that can reduce the error value over time. A traditional PID strategy is implemented in our simulations to control the quadcopter. However, the framework is extensible to other control algorithms of increasing complexity. In any case, as reported in [15] and [16], PID control is the most widely implemented in the industrial process, as it is a good compromise between robustness and performance for UAS autopilot design. For different approaches to PID UAV control, the reader may refer, for example, to [17]. In particular, we consider a cascade PID controller to maintain a constant position, altitude, and attitude at different distances from the wall.

To the authors' knowledge, there are no other publications to report on this type of approach in the context of UAS flights. However, there are some examples of PID-controlled CFD simulations [18], in which the authors propose a new method of tuning the PID controller parameters using CFD simulation for a greenhouse climate control system, avoiding the implementation of the sensors model. A similar CFD-based ventilation test method is presented in [19] for a conditioned room model to evaluate the ventilation system and control performance. On the other hand, several

authors simulated quadcopters with some degrees of freedom but without a control strategy or the generality of a 6-DOF simulation. For example, some authors [20] present a similar approach in urban air mobility using loosely-coupled high-fidelity CFD simulations with the reduced-order model CAMRAD-II to achieve a trimmed cruise condition.

The main objective of this work is to present an innovative approach to simulate precision maneuvers with a higher fidelity model compared to the simplified propulsive models traditionally used for control applications. The method includes a control system coupled with a Computational Fluid Dynamics model that helps analyze critical scenarios such as ground/wall effect near obstacles or wind gusts disturbances. Thus, the research contributes to increasing the safety and reliability of UAS missions, and improving the tuning of PID controller gains.

The paper structure is the following. Section II proposes the methodology and tools, including a detailed UAS dynamic model, the PID control law, and the CFD modeling. It also contains the simulation results, comparing simplified and realistic dynamics and the environment for two case studies. Section III contains the simulation results of the quadcopter in wall effect. We present two studies, one in which the UAS is fixed and the forces and moments are computed at different wall distances and another in which the UAS uses a PID algorithm to maintain a hovering position. Finally, we outline our conclusions and future activities in Section IV.

II. Methodology and tools

This section illustrates the proposed methodology with the mathematical formulation and the underlying numerical tools. Initially, a simple horizontal translation is shown as a validation case. Then a critical maneuver, hovering in the neighborhood of the wall, is analyzed in detail. The challenge is to evaluate the ability of the discussed control algorithm to maintain a constant position, altitude, and attitude at different distances from the wall.

A. Quadrotor dynamics

A six-degree-of-freedom (DOF) UAS rigid body model is implemented in a MATLAB/Simulink environment to simulate the desired maneuvers and tune the controller parameters. For this work, a quadrotor model is chosen. This UAS represents an under-actuated system with four inputs, which are the angular velocities of four rotors. They are controllable in position and attitude dynamics through thrust and torque generation. The model of a multi-rotor is described in detail in [21]. In this research, the "+" (cross) quadrotor orientation is considered, where the drone has two rotors parallel to the body x-axis (rotors 1 and 3 with counterclockwise rotation) and two rotors parallel to the body y-axis (rotors 2 and 4 with clockwise rotation), as shown in Figure 1 with the main quadrotor parameters taken as a reference. As mentioned before, four control inputs influence the quadrotor dynamics, u_1 the sum of all rotor forces, u_2 the rolling moment generated along y_b, u_3 the pitching moment generated along x_b, and u_4 the yaw moment around z_b. A propulsive model relating the thrust and torque of each rotor ($i = 1, ..., 4$) is introduced as a function of the rotation rate (ω_i) to obtain these forces and moments. In the simplified model, a constant coefficient model for k_T and k_D, thrust
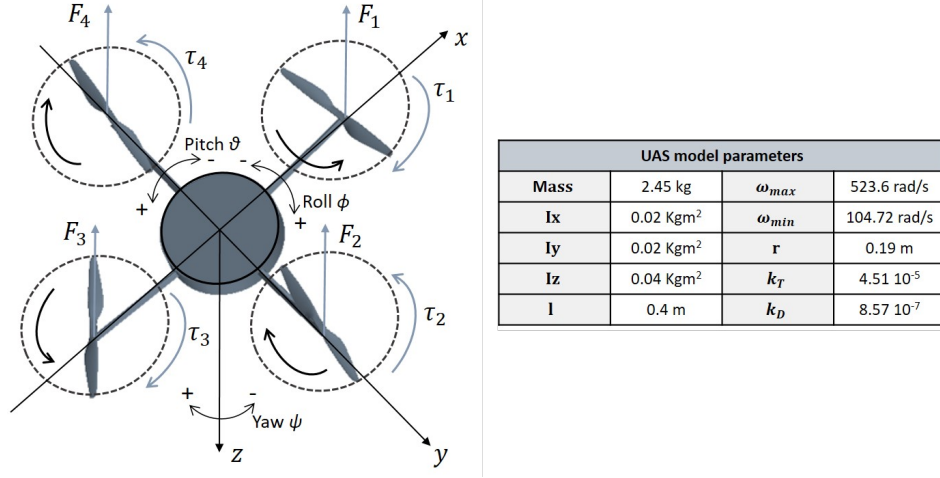
Fig. 1   Forces and torques on the quadrotor in the body frame and parameters used in the simulation.

and torque coefficient, respectively, is used as shown in Eqs.1 and 2.

$$F_i = k_T \, \omega_i^2 \tag{1}$$

$$\tau_i = (-1)^{i+1} k_D \, \omega_i^2 \tag{2}$$

Combining the rotor forces and moments as defined in Figure 1, the control algorithm, discussed in II.B, provides four control inputs (u_1, u_2, u_3, u_4) and the rotor rotation rate required for each motor can be calculated using Eq. 3. The rotors rotation rates (ω_1, ω_2, ω_3, ω_4) will be the input values of the CFD model.

$$
\begin{bmatrix} \omega_1^2 \\ \omega_2^2 \\ \omega_3^2 \\ \omega_4^2 \end{bmatrix}
=
\begin{bmatrix}
k_T & k_T & k_T & k_T \\
0 & -lk_T & 0 & lk_T \\
lk_T & 0 & -lk_T & 0 \\
k_D & -k_D & k_D & -k_D
\end{bmatrix}^{-1}
\begin{bmatrix} u_1 \\ u_2 \\ u_3 \\ u_4 \end{bmatrix}
\tag{3}
$$

B. PID control design

A Proportional-Integral-Derivative (PID) controller is implemented to test the effectiveness in combination with CFD simulations, not forgetting the limit of the computational cost. This control law is popular because of its simplicity, robustness, and effectiveness in forcing the controlled variable $y(t)$ to follow as closely as possible a reference variable $r(t)$ defined by the guiding law [22]. As a feedback control, the system acquires the measurement of the controlled variable to stabilize the system, reducing the error $e(t) = r(t) - y(t)$ between the reference and the measured variable. The control
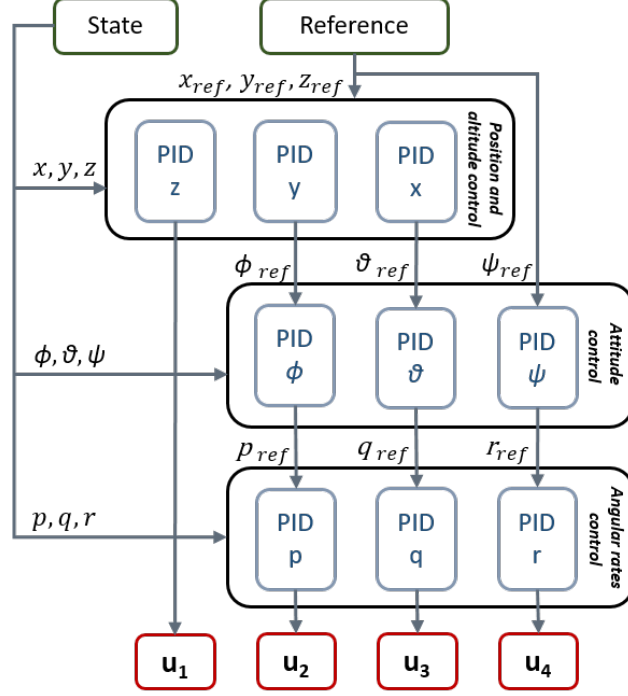
Fig. 2 Robust cascade PID position and attitude control.

signal *u(t)* becomes

$$u(t) = K_P e(t) + K_I \int e(\tau)d\tau + K_D \frac{d}{dt}e(t) \tag{4}$$

where K_P is the proportional gain, K_I is the integral gain, and K_D is the derivative gain. Moreover, adjusting these control parameters to reach the reference in a finite time is relatively easy to accomplish the required performance in terms of stability, steady-state error, and convergence time.

A robust cascade PID control algorithm to track position and the yaw angle (x_{ref}, y_{ref}, z_{ref}, ψ_{2ref}) has been developed, as shown in Figure 2. Inputs to the control logic are (x, y, z), (ϕ, θ, ψ) and (p, q, r) in body frame. Sensors and noises are not considered in this model.

C. CFD analysis

The commercial CFD software STARCCM+ [23] was used to develop a 6-DOF computational model of a quadrotor equipped with the PID controller previously described in Section II.B. An overset grid interface strategy allows the UAS to move within a background grid. Simulations are executed in a closed cube environment with a height, width, and depth of 20 meters, as shown in Figure 3. Using such a large domain is possible without needing too many cells since the background mesh is very coarse. An automatic Adaptive Mesh Refinement (AMR) algorithm refines the background mesh using the interface with the body grid as a trigger function, which moves in solidarity with the quadcopter, as shown in Figure 3. The adaptive mesh refinement occurs every ten integration steps to limit the computational cost. The

simulation environment remains a cube for the wall effect simulations shown in Section III. The UAS is moved towards a wall and oriented adequately depending on the desired configuration. In this case, avoiding the overhead of using an AMR strategy is preferable, and a volumetric refinement is performed around the UAS.
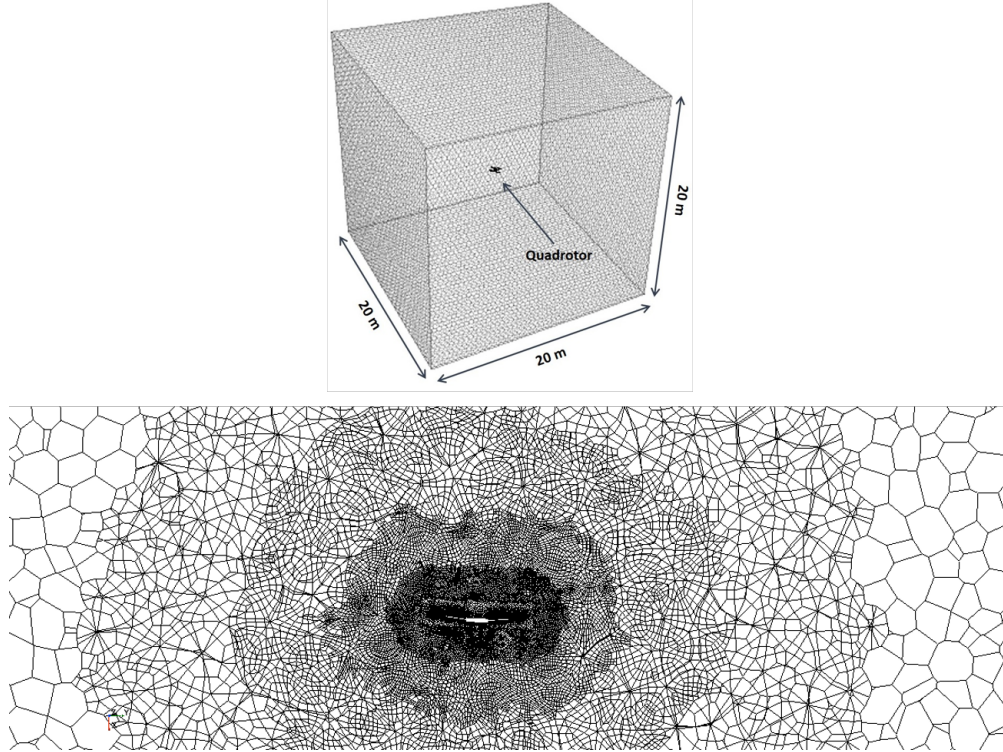

Fig. 3   CFD simulation domain and the computational grid with adaptive mesh refinement tracking the near-body grid.

A sliding grid approach models the rotors' motion [24] inside the body overset grid. The time step is defined to allow a maximum rotation angle of 3° per temporal iteration at the highest angular velocity defined in the table in Figure 1. This time step is around $10^{-4}s$, so the simulated physical time is limited depending on the computational resources. The adopted time-integration scheme is implicit and second-order accurate, and the spatial discretization is also second-order. As a turbulence model, we use the URANS one-equation Spallart-Allmaras model [25]. The grid adopted in this work is under-resolved (5 million points) to simulate aerodynamic rotor-rotor interactions or the wake breakdown in detail. However, its refinement is sufficient to describe the coupling between rotor aerodynamics and quadrotor dynamics. Such a capability provides our simulations with a noticeable advantage compared to the simplified propulsive model usually employed in dynamic simulations, which relies on constant thrust and torque coefficients, as shown in Eq. 3. We verified the scalability of such an approach to larger grids by running the simulations on a 5 million and a 10 million cells grid. The results showed an under-linear increase in CPU time due to the reduced importance of the overhead that the 6-DOF solver adds to the simulation. That is an aspect that improves the performance of parallel computing. The link between the controller and the CFD model depends on the rotation rates at each time step, and the

framework includes an input file that allows the definition of different waypoints.

Figure 4 illustrates our virtual control test strategy. In particular, the process controller, being a feedback system, computes the error between a reference signal and an actual state vector obtained from the CFD model. Its output, namely forces and torques, is converted in rotation rates according to Eq. 3 and enters directly into the virtual simulator.

We conducted the simulations using the 32 cores of an Intel Xeon Scalable Processors Gold 6130 2.10 GHz. The computational cost of the 6-DOF maneuvers presented in this paper, with a duration of 1.5 seconds, is around 5000 CPU hours. These simulations were performed with the 5 million grid. On the other hand, the static overset grid simulations are performed with the 10 million grid with a computational cost of around 9000 CPU hours.
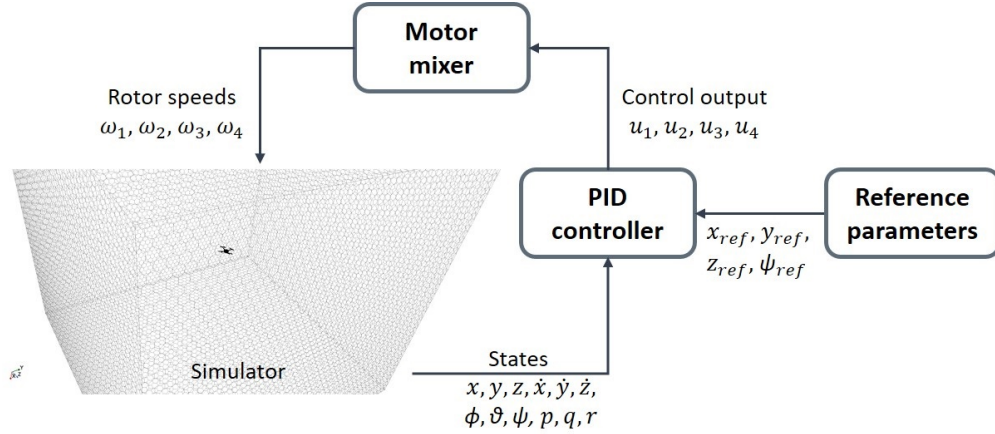

Fig. 4   Configuration of the virtual UAS control test system.

D. Numerical Verification: Quadcopter in horizontal translation

Our CFD/PID simulation framework's results are compared with a simplified model for a simple test case. In particular, a horizontal translation of 20 cm on the x-axis, maintaining altitude, is simulated. The active control must move the UAS to the desired position while contrasting the gravity force. We compare the simplified Simulink model and the CFD simulation to evaluate seldom-captured non-linear aerodynamic and propulsion effects. To show the translation along the x-axis NED, we present the relevant states x and θ, the pitch angle, in Figure 5. The two states are comparable in both models, and minor discrepancies are due to the transient of the rotors and the fact that the fluid force on the multicopter's frame is also computed.

Finally, we show some images from the CFD simulation in Figure 6, where one can see the simulated advancing maneuver of the quadcopter. It is possible to see the downwash velocities and the vehicle's attitude. Initially, the quadcopter has a negative pitch angle to accelerate the vehicle to the desired position. Then, a higher thrust, revealed by the increased downwash speeds in rotor 1, helps increment the pitch angle to positive values, as shown in Figure 5, in an attempt to compensate for the positive velocity that the vehicle has acquired. The last images show that the UAS asymptotically regains a hovering position at an x coordinate of 20 cm. A detailed verification of this maneuver was
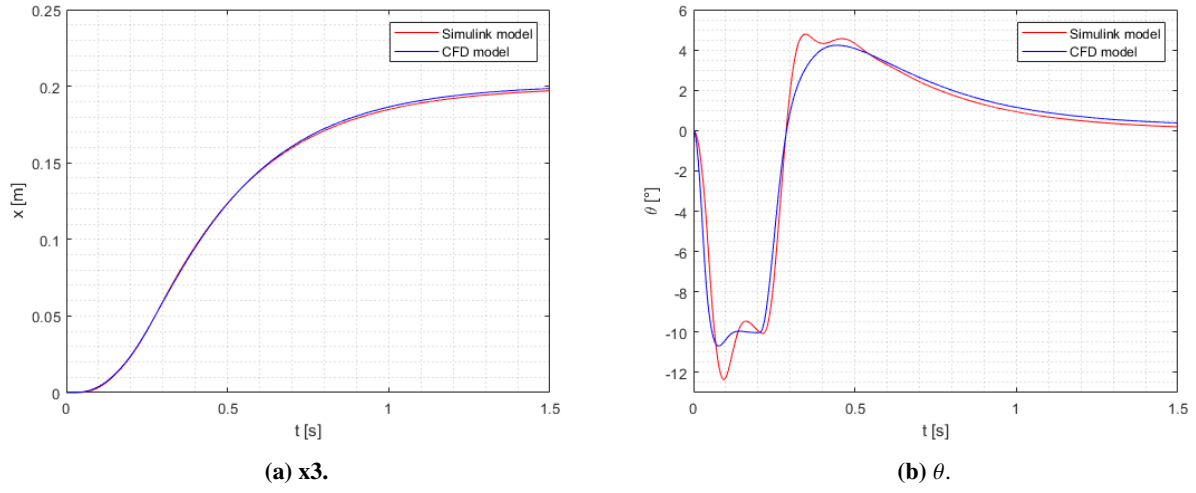
(a) x3.

(b) θ.

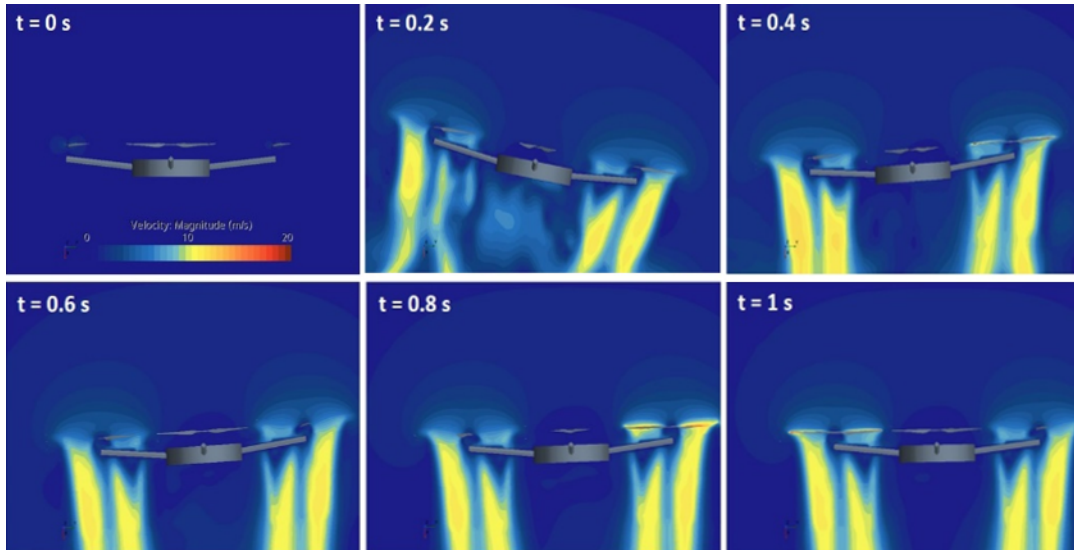Fig. 5   Comparison of x-position and θ for the two models.

Fig. 6   Visualization of the velocity magnitude field obtained with CFD during the quadrotor maneuver.

8

presented in [26].

III. Quadcopter in Wall Effect

This section presents a numerical analysis of a quadcopter operating in wall effect using CFD simulations. We present two types of analysis, static simulations at a fixed distance from the wall and 6-DOF simulations of the same quadcopter using a PID controller that compensates for the disturbances caused by the wall. Figure 7 shows a sketch of the UAS position relative to the wall used for the static simulations. This configuration is known to maximize the wall effects on the quadcopter [12]. On the other hand, dynamic simulations have been performed in the configuration described in Figure 8. In this case, we maintain a hover position with the UAS flying in a '+' configuration parallel to the wall. These maneuvers cannot be reproduced with a classical simplified propulsive model as it would not be able to account for near-wall effects on the quadcopter dynamics. Therefore, this CFD/PID framework becomes essential to understand this complex coupled aerodynamic/dynamic phenomenon as experimental testing risks the loss of the UAS, incurring high costs. In this regard, using CFD simulations during the design of experiments seems helpful in improving the campaign's safety.
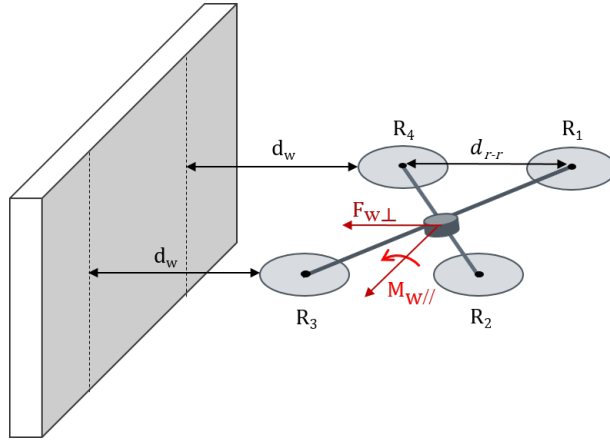

Fig. 7   Quadrotor near a wall in configuration 1.

1. Simulations with a Fixed UAS

This section assesses the magnitude of the forces acting on the UAS at three different wall distances. These simulations are performed with a fixed UAS but provide information on future dynamic behavior. The main effects that near-wall operating UAS experiences are a wall-normal force that tends to attract the multicopter to the wall and a roll moment that tends to flip the quadcopter towards the wall as shown in [12]. Table 1 shows the effect of reducing the tip wall clearance. It is clear how these forces and moments increase as we reduce the distance to the wall. This generates an unstable dynamic situation as the attraction force and tilt moments tend to reduce the wall distance creating a super-linear reduction in wall distance. Interestingly, as these simulations have been performed with a zero tilt angle,
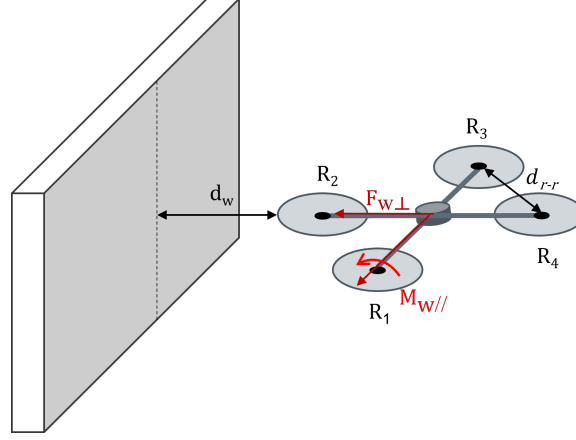
9

Fig. 8   Quadrotor near a wall in configuration 2.

the inherent coupling between the tilt angle and the thrust orientation is not the reason for the attraction force.

In order to understand the underlying physical phenomena that generate these forces and moments, Figure 9 shows the velocity contours and streamlines in a vertical plane normal to the wall that contains the centers of two rotors. A simple interpretation of how the flipping moment is created can be deduced from the differences in the flow field around the rotors. The rotors placed near the wall show an increased inflow velocity due to the blockage of the wall. This decreases the effective angles of attack, slightly reducing the thrust of these compared with the rotor, which is placed far away from the wall and does not suffer this blockage. These minor differences in thrust can generate non-negligible moments due to the separation between rotors, as shown in Table 1. This effect is accentuated when the wall clearance is reduced. On the other hand, the attraction force is caused by the reduced change in horizontal momentum seen across the rotor closer to the wall due to the more vertical inflow direction compared to the rotor positioned further away from the wall, appreciated in figure 9.

These simulations require around 1.5 seconds to achieve a statistically converged solution. This corresponds approximately with 100 rotor revolutions. This represents around an order of magnitude higher than the number of revolutions required to achieve converged forces and moments in an isolated rotor simulation. This shows that even though the wall effect creates a dangerous situation for multicopter flights, its relatively slow dynamics could help the ability of controllers to handle this kind of operation safely.

Table 1   Influence of tip clearance in time-averaged forces and moments on the Quadcopter.

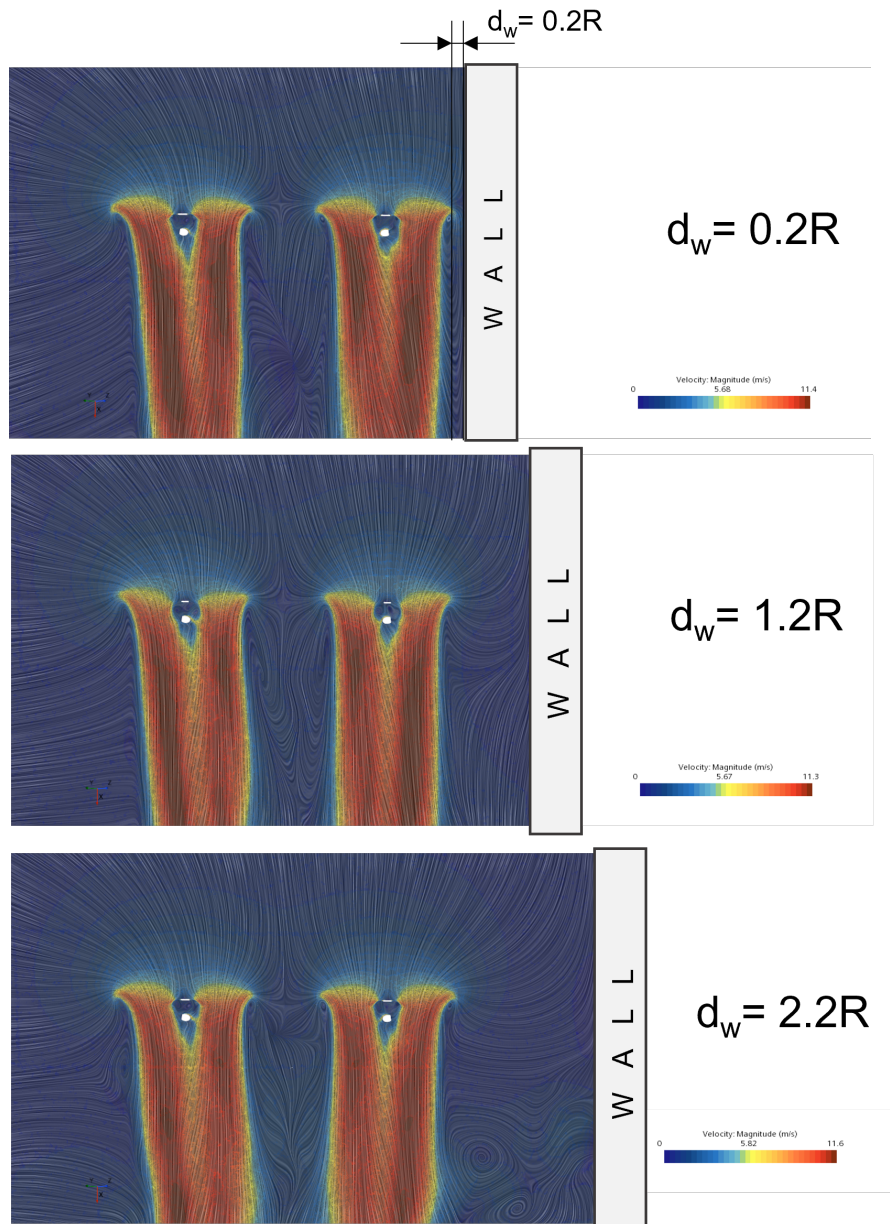| Tip-Wall Clearance (Rotor Radii)	Wall-Normal force (N)	Roll Moment (Nm)
0.2 R	0.098	0.075
1.2 R	0.054	0.067
2.2 R	0.036	0.045

Fig. 9 **Influence of tip clearance in the fluid flow around the quadcopter.**

2. 6-DOF UAS simulations

In this section, a hovering condition near a wall is analyzed. Simulations without the control algorithm activated reveal the progressive dragging of the vehicle toward the wall. Therefore, different distances from the wall are simulated to understand the UAS behavior sensitivity to this parameter. In both cases, we found that the control algorithm could find a trimmed position with a roll angle orienting the positive normals of the rotors away from the wall. A small thrust component compensates for the suction effect towards the wall that the vehicle experiences.

In particular, we performed two simulations with the nearest rotor placed at 5 cm and 10 cm of the wall, using configuration 2 as shown in Figure 8. Figure 10 shows the evolution of the roll angles during the mission. In the case of larger wall clearance, the trimmed roll angle is -0.38 degrees, which decreases to -0.45 degrees for the smallest wall clearance. Even though the absolute values are small, they are sufficient to compensate for the wall suction force shown in the previous section. The roll angle increases by around 20% when the wall distance is reduced. Considering that for these small angles, we can assume that the lateral force is proportional to the thrust's and the angle's product, the wall's suction force would have also increased by 20%. The PID controller also compensates for the wall-induced roll moment by slightly increasing the rotation rate of the rotor closer to the wall (Rotor-2) compared to its opposite rotor (Rotor-4). This effect can be appreciated in Figure 11.
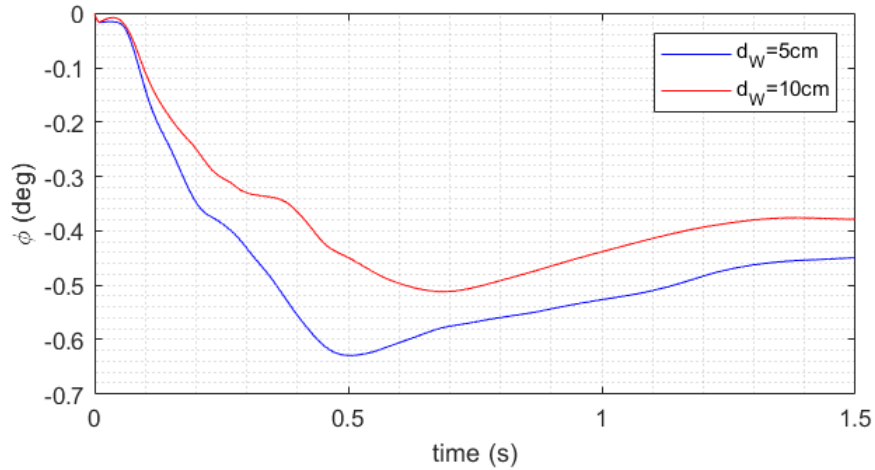

Fig. 10   Roll angle of the quadcopter hovering in configuration 2 at different wall distances.

These results show how beneficial CFD simulations can be in understanding the wall effect in which multicopters are obliged to work for several applications and the coupling with the UAS controller. Furthermore, it will help us to
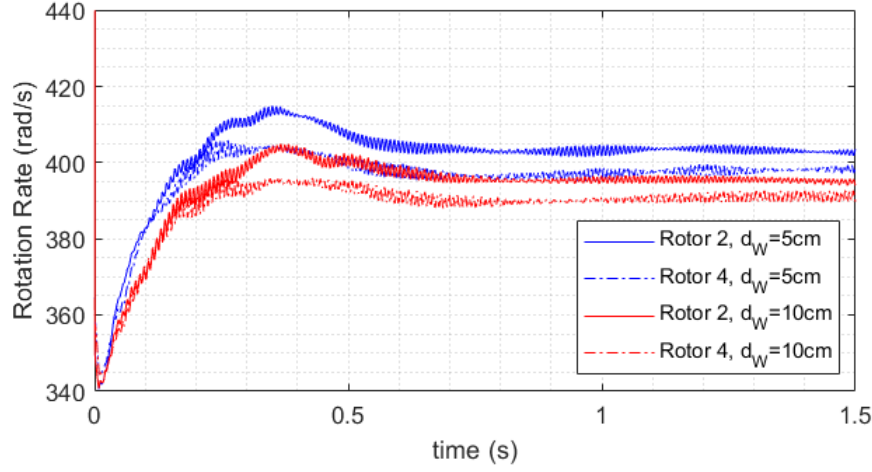
Fig. 11   Rotation rates of rotors 2 and 4 hovering in configuration 2 at different wall distances.

plan future experimental activities that will help to validate this model and to develop simplified propulsive models which are capable, up to some degree, of capturing the disturbances generated by the wall.

IV. Conclusions and future works

In this paper, we presented a model to simulate the flight of a quadcopter that combines a PID controller with a CFD simulation to reproduce UAS maneuvers accurately. This innovative strategy has produced coherent results compared with simplified propulsion and dynamics. This CFD/PID framework simulation framework was numerically verified in a simple case, such as a horizontal translation, where a simplified propulsive model could perform reasonably accurately. Then we employed the verified model to investigate the dynamic behavior of a multicopter hovering in the neighborhood of a wall.

We initially studied the wall effect with a fixed quadcopter to understand the aerodynamic interaction of the flow generated by the rotors and the wall. We verified that the two primary disturbances that the presence of the wall produces are a suction force toward the wall and a rolling moment that tends to point the rotor normals toward the wall. The rolling moment is probably associated with a slightly reduced thrust caused by the blockage of the wall and the suction force with the fact that the change of lateral momentum across the disk is reduced due to the more vertical streamlines shown near the wall. We also detected that the characteristic time for the forces to converge is around 1.5 seconds, and these are relatively small, which suggests that the wall-induced disturbance has a small frequency.

13

Finally, the 6-DOF CFD simulations revealed that the controller could achieve a trimmed hovering position at a slight negative roll angle, pointing the rotor normals away from the wall and compensating in this way for the suction force. An increase in the rotation rate of the near-wall rotor compensates for the previously discussed wall-induced moment. The trim angle becomes more negative as we reduce the distance toward the wall.

As further work, we will perform experimental testing to validate the model. We aim to assess the model's fidelity by comparing CFD-based virtual flight testing and actual flight logs. Furthermore, we plan to simulate non-hovering missions parallel to the wall to assess the ability of the controller and maintain the desired trajectory. We will also assess the influence of the frequency at which the controller works on the ability to respond to wall effect disturbances.

Acknowledgment

References

[1] Idrissi, M., Salami, M., and Annaz, F., "A Review of Quadrotor Unmanned Aerial Vehicles: Applications, Architectural Design and Control Algorithms," *Journal of Intelligent & Robotic Systems*, Vol. 104, No. 2, 2022, pp. 1–33.

[2] Mohamed, N., Al-Jaroodi, J., Jawhar, I., Idries, A., and Mohammed, F., "Unmanned aerial vehicles applications in future smart cities," *Technological Forecasting and Social Change*, Vol. 153, 2020, p. 119293.

[3] Radoglou-Grammatikis, P., Sarigiannidis, P., Lagkas, T., and Moscholios, I., "A compilation of UAV applications for precision agriculture," *Computer Networks*, Vol. 172, 2020, p. 107148.

[4] Bloise, N., Primatesta, S., Antonini, R., Fici, G. P., Gaspardone, M., Guglieri, G., and Rizzo, A., "A survey of unmanned aircraft system technologies to enable safe operations in urban areas," *2019 International Conference on Unmanned Aircraft Systems (ICUAS)*, IEEE, 2019, pp. 433–442.

[5] Zhang, Y., Chen, Z., Zhang, X., Sun, Q., and Sun, M., "A novel control scheme for quadrotor UAV based upon active disturbance rejection control," *Aerospace Science and Technology*, Vol. 79, 2018, pp. 601–609.

[6] Matus-Vargas, A., Rodríguez-Gómez, G., and Martínez-Carranza, J., "Aerodynamic disturbance rejection acting on a quadcopter near ground," *2019 6th International Conference on Control, Decision and Information Technologies (CoDIT)*, IEEE, 2019, pp. 1516–1521.

[7] Matus-Vargas, A., Rodriguez-Gomez, G., and Martinez-Carranza, J., "Ground effect on rotorcraft unmanned aerial vehicles: a review," *Intelligent Service Robotics*, Vol. 14, No. 1, 2021, pp. 99–118.

[8] Kazim, M., Azar, A. T., Koubaa, A., and Zaidi, A., "Disturbance-rejection-based optimized robust adaptive controllers for UAVs," *IEEE Systems Journal*, Vol. 15, No. 2, 2021, pp. 3097–3108.

[9] Bolandi, H., Rezaei, M., Mohsenipour, R., Nemati, H., and Smailzadeh, S. M., "Attitude control of a quadrotor with optimized PID controller," 2013.

[10] Shi, Q., Pan, Y., He, B., Zhu, H., Liu, D., Shen, B., and Mao, H., "The airflow field characteristics of UAV flight in a greenhouse," *Agriculture*, Vol. 11, No. 7, 2021, p. 634.

[11] Paz, C., Suárez, E., Gil, C., and Baker, C., "CFD analysis of the aerodynamic effects on the stability of the flight of a quadcopter UAV in the proximity of walls and ground," *Journal of Wind Engineering and Industrial Aerodynamics*, Vol. 206, 2020, p. 104378.

[12] Conyers, S. A., "Empirical evaluation of ground, ceiling, and wall effect for small-scale rotorcraft," Ph.D. thesis, University of Denver, 2019.

[13] Du Mutel de Pierrepont, I. D., Capello, E., Vilardi, A., Parin, R., et al., "Experimental evaluation of Wall Effect for small UAVs in Climate-Controlled Environments," *2022 IEEE 9th International Workshop on Metrology for AeroSpace (MetroAeroSpace)*, IEEE, 2022, pp. 119–123.

[14] Robinson, D. C., Chung, H., and Ryan, K., "Computational investigation of micro rotorcraft near-wall hovering aerodynamics," *2014 International Conference on Unmanned Aircraft Systems (ICUAS)*, IEEE, 2014, pp. 1055–1063.

[15] Salih, A. L., Moghavvemi, M., Mohamed, H. A., and Gaeid, K. S., "Flight PID controller design for a UAV quadrotor," *Scientific research and essays*, Vol. 5, No. 23, 2010, pp. 3660–3667.

[16] Wang, P., Man, Z., Cao, Z., Zheng, J., and Zhao, Y., "Dynamics modelling and linear control of quadcopter," *2016 International Conference on Advanced Mechatronic Systems (ICAMechS)*, IEEE, 2016, pp. 498–503.

[17] Szafranski, G., and Czyba, R., "Different approaches of PID control UAV type quadrotor," 2011.

[18] Xiao, H., Feng, L., and Zhi, Y., "Tuning the PID parameters for greenhouse control based on CFD simulation," *2013 Second International Conference on Agro-Geoinformatics (Agro-Geoinformatics)*, IEEE, 2013, pp. 485–489.

[19] Sun, Z., and Wang, S., "A CFD-based test method for control of indoor environment and space ventilation," *Building and Environment*, Vol. 45, No. 6, 2010, pp. 1441–1447.

[20] Ventura Diaz, P., and Yoon, S., "High-Fidelity Simulations of a Quadrotor Vehicle for Urban Air Mobility," *AIAA SCITECH 2022 Forum*, 2022, p. 0152.

[21] Valavanis, K. P., and Vachtsevanos, G. J., *Handbook of Unmanned Aerial Vehicles-5 Volume Set*, New York, NY, USA: Springer, 2014.

[22] Becce, L., Bloise, N., and Guglieri, G., "Optimal Path Planning for Autonomous Spraying UAS framework in Precision Agriculture," *2021 International Conference on Unmanned Aircraft Systems (ICUAS)*, IEEE, 2021, pp. 698–707.

[23] Siemens, P., "STAR-CCM+ User Guide Version 14.06," *Siemens PLM software Inc*, 2019.

[24] Carreño Ruiz, M., Scanavino, M., D'Ambrosio, D., Guglieri, G., and Vilardi, A., "Experimental and numerical analysis of multicopter rotor aerodynamics," *AIAA Aviation 2021 Forum*, 2021, p. 2539.

[25] Spalart, P., and Allmaras, S., "A one-equation turbulence model for aerodynamic flows," *30th Aerospace Sciences Meeting and Exhibit*, 1992. https://doi.org/10.2514/6.1992-439.

[26] Carreño Ruiz, M., Bloise, N., Capello, E., D'Ambrosio, D., and Guglieri, G., "Assessment of Quadrotor PID Control Algorithms using six-Degrees of Freedom CFD simulations," *2022 61st IEEE Conference on Decision and Control (CDC)*, 2022.